

Lipid Nanoparticles: Tumor-targeting Nanocargos for Drug and Contrast Agent Delivery

I. Texier*, T. Delmas**, F. Navarro*, J. Mérian***, J. Gravier*, J.S. Thomann*, E. Heinrich*, F. Mittler*, R. Boisgard**, B. Tavitian**, S. Dufort****, J.L. Coll****, J. Bibette**, P. Boisseau*, A.C. Couffin*

*CEA-LETI MINATEC/ DTBS, 17 avenue des Martyrs, 38054 Grenoble Cedex 9, France, isabelle.texier-nogues@cea.fr

**LCMD, ESPCI, 10 rue Vauquelin, 75231 Paris cedex 5, France, jerome.bibette@espci.fr

***CEA Orsay SHFJ, 4 place Général Leclerc, 91401 Orsay Cedex, France, bertrand.tavitian@cea.fr

****INSERM U823, Institut Albert Bonniot, 38706 La Tronche Cedex, France, jean-luc.coll@ujf-grenoble.fr

ABSTRACT

A new technology for the encapsulation of lipophilic molecules -both drugs and contrast agents- has been developed, based on oil-in-water nanoemulsions. Physico-chemical characterizations of the nanoparticles evidence highly stable lipid nanoemulsions with amorphous core of temperature- and composition- tunable viscosity. Particles display low *in vitro* cytotoxicity ($IC_{50} > 300 \mu\text{g/mL}$ of lipids), and high tolerance *in vivo*. They can be efficiently loaded with hydrophobic to amphiphilic molecules, such as fluorescent dyes for tumor labeling, photosensitizers for phototherapy, or chemotoxic drugs. The presence of PEGylated surfactants in the particle coating ensures a good *in vivo* stealthiness, as assessed by their biodistribution recorded using fluorescence imaging and radioactivity counting (^{14}C and ^3H particle labeling). The lipid nanoparticles can moreover be functionalized by tumor-targeting ligands, such as the cRGD peptide, to improve specific tumor cell accumulation.

Keywords: lipid nanoparticles, drug delivery, fluorescence imaging, oncology

1 INTRODUCTION

Both drug delivery and molecular imaging fields seek for more efficient targeting of drugs and contrast agents in pathological area, especially through the help of nanocargos. The nanometer size (30-200 nm) seems particularly attractive for oncology: for instance, passive targeting of nanoparticles to tumor sites is favored by the leaky vasculature of tumors along with the low lymphatic drainage in the tumor interstitium (EPR effect) [1]. Among a wide variety of nanocargos [2, 3], lipid-based particles present several advantages: their ingredients are mostly low cost lipids and biocompatible surfactants, their manufacturing process is versatile and up-scalable [4, 5].

A new technology for the encapsulation of lipophilic molecules -both drugs and contrast agents dedicated to

chemotherapy, phototherapy, or fluorescence imaging in oncology- has been developed, based on oil-in-water nanoemulsions (Figure 1) [6-9]. The main previously reported drawback of these objects -namely intrinsic poor colloidal stability- has been overcome by the use of a complex mixture of core lipids and surfactants, bringing entropy mixing stabilization to the physico-chemical system [7]. The designed lipid nanoparticles, termed as "Lipidots™", have been characterized for i) their physico-chemical properties; ii) their cytotoxicity; iii) their biodistribution. Their loading with hydrophobic to amphiphilic molecules, such as fluorescent dyes for tumor labeling, photosensitizers for phototherapy, or chemotoxic drugs, has been explored for oncology applications. The present report summarizes the results obtained so far and the future prospects for Lipidots™ technology.

2 RESULTS AND DISCUSSION

2.1 Lipidots™ Design and Physico-Chemical Characterization

Lipidots™ are composed of a lipid core, mixture of soybean oil and a wax at different ratios, and a surfactant shell, mixture of phospholipids and PEGylated surfactants (Figure 1). Their ingredients are bioabsorbable, since most of them enter natural lipid metabolism, and are biocompatible, as they are already FDA approved for human-use.

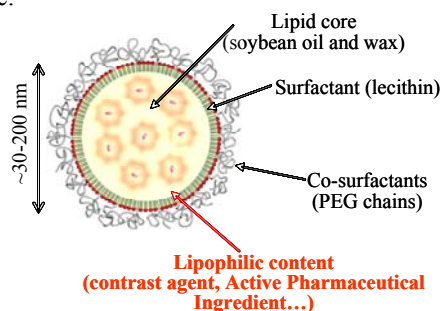


Figure 1: Schematic representation of Lipidots™.

The particles are processed by ultrasonication. Batches of particles with specified diameter can be obtained depending on the lipid and surfactants ratios, as previously described [6, 7, 9]. Thorough physico-chemical characterizations of the nanoparticles have been carried out using different techniques (Dynamic Light Scattering, Differential Scanning Calorimetry, ^1H NMR).

Dynamic Light Scattering (DLS) is used to measure the particle hydrodynamic diameter in PBS or saline dispersions, as well as their time-evolution during storage. Figure 2 demonstrates that very-long term can easily be achieved, even at 40°C . Lipid emulsions are known to be destabilized because of coalescence and/or Ostwald ripening. The nanometric size of the lipid droplets prevents coalescence destabilization [10]. We recently evidenced that Ostwald ripening could be prevented by the use of complex mixtures for both the core lipids and the shell surfactants, bringing entropy mixing stabilization to the physico-chemical system [7]. This should account for the long-term stability observed for LipidotsTM.

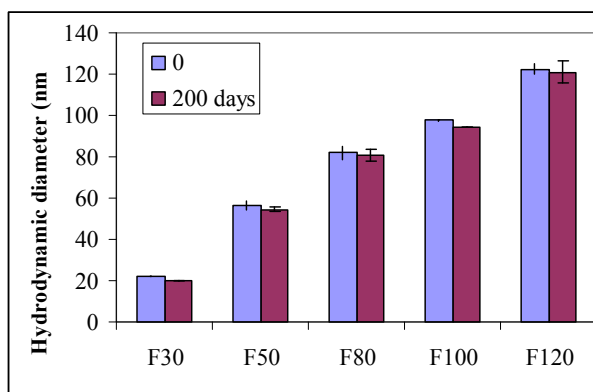


Figure 2: Long-term stability during 40°C storage of five lipid nanoparticle batches with different nominal sizes (FXX indicates XX nm diameter particles).

The internal physical state of the particle core has been characterized by Differential Scanning Calorimetry (DSC) and ^1H NMR analysis. DSC thermograms display no evidence of any crystallization event in the particle dispersions, even after prolonged storage at 4°C (up to 8 months), and for compositions for which the core is 100% wax, which crystallizes as a bulk below 35°C . The particle lipid core therefore appears to be in an amorphous state in a wide range of temperature and lipid core compositions. This amorphous state should favor long-term encapsulation and homogeneous release of active ingredients from the LipidotsTM core. ^1H NMR experiments are used to probe the viscosity of the particle core. An increase of the lipid core wax ratio or decrease of the temperature broadens ^1H NMR peaks attributed to core components (hydrocarbon chains and phospholipid choline heads), in comparison to PEG surfactants chains, able to freely move in aqueous buffer. Therefore, core wax composition and temperature appear to be parameters able to control the lipid core viscosity [6].

2.2 LipidotsTM Cytotoxicity and Biodistribution

LipidotsTM cytotoxicity is assessed by WST-1 assay using NIH 3T3 murine fibroblasts (Figure 3). The lipid nanoparticles display *in vitro* cytotoxicity with an $\text{IC}_{50} \approx 300 \mu\text{g/mL}$ of lipids, higher or similar to reported values for other nanosystems such as liposomes or Solid Lipid Nanoparticles [11]. Very surprisingly, cell viability for different particle sizes scales as nanoparticle mass (core lipids and surfactants) (Figure 3), and not as the particle total area, as often encountered for nanomaterials. It could be indicative that the cell cytotoxicity is in fact mainly driven by the more cytotoxic of the components entering the particle composition (in this case the PEG surfactant, however approved for human use), than by the nanoformulation effect.

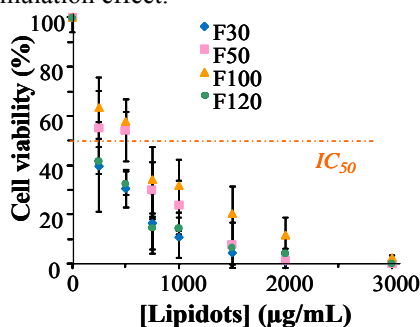


Figure 3: LipidotsTM cytotoxicity after 24 hours incubation at 37°C in the presence of 3T3 fibroblasts.

In vivo tolerance of 50 nm-diameter LipidotsTM is assessed by a rat study following unique IV injection of a high dose of nanoparticles (150 mg lipids / kg). 100% survival rate is observed after 5 weeks, with normal behavior, normal body weight increase, no food consumption fluctuations and absence of any suffering.

The biodistribution of 50 nm-diameter LipidotsTM in FVB mice is investigated encapsulating in the lipid core ^{14}C -cholesteryl oleate (CO) and ^3H -cholesteryl-hexadecyl-ether (CHE) and performing radioactivity counting. The injection of the *free* radiotracers in FVB mice leads to their accumulation mainly in lungs, and less extendingly in spleen and liver. On the contrary, the injection at the same dose of the radiotracers encapsulated in the LipidotsTM leads to a different biodistribution, evidencing a nanovectorization effect of the particles (Figure 4). Radioactivity decays in plasma with a half life of about 45 minutes, and is uptaken mainly in liver. The two tracers, one of which can be metabolized (^{14}C -CO), follow similar biodistribution pattern up to ≈ 2 hours after injection, which could be indicative that the LipidotsTM keep its integrity during this lapse of time *in vivo*. Liver uptake seems to be mainly due to accumulation of the particles in hepatocytes rather than macrophages, since very low tracer levels are detected in spleen and lungs, other organs known for macrophage homing. The subsequent decay of ^{14}C -CO liver level indicates a metabolization of the tracer by the hepato-

biliary pathway. Therefore, the dense nanoparticle coating with PEGylated surfactants seems to ensure Lipidots™ a good *in vivo* stealthiness and prevents their massive macrophage uptake after IV injection, as reported previously for other systems [12].

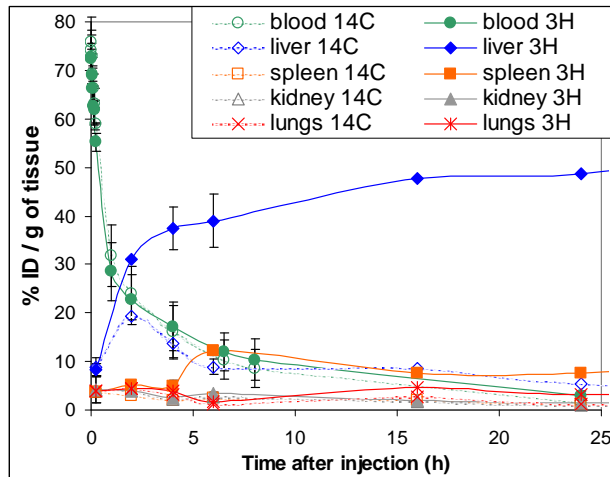


Figure 4: Biodistribution of Lipidots™.

2.3 Lipidots™ Loading

Lipidots™ can be efficiently loaded with different hydrophobic to amphiphilic molecules, with $\log P > 2$. Figure 5 summarizes examples of molecules that have been successfully loaded within the nanoparticles. Fluorescent organic dyes can be used for imaging applications, such as *in vivo* tumor labeling [9], or as models to assess the encapsulation and release behavior of the Lipidots™. Depending on the solubility and affinity of the molecules to be loaded within the lipid core, high loading ratios can be achieved (for instance mTHPC, a photosensitizer, can be loaded up to 7 % w/w of lipids). Since the nanoparticles are stably dispersed in aqueous buffers, Lipidots™ loading also provides the encapsulated active ingredients with a high solubility and long-term stability in water. For instance, high fluorescence quantum yields and reduction of the photobleaching rates are observed for dyes encapsulated in the lipid nanoparticles [9], providing highly fluorescent labels for *in vitro* and *in vivo* detection.

2.4 Lipidots™ Applications in Oncology

The EPR effect, ie passive targeting of nanoparticles to tumor sites favored by the leaky vasculature of tumors along with the low lymphatic drainage in the tumor interstitium, has been extensively described in the literature for a wide variety of nanocarriers [1].

Passive tumor uptake of 50 nm-diameter Lipidots™ has been studied for a variety of tumor models implanted subcutaneously in *Nude* mice using DiD-loaded Lipidots™ [8, 9]. DiD is a near-infrared emitting organic dye, which fate can be assessed non invasively using fluorescence imaging. Figure 6 displays the fluorescent images obtained 24 hours

after IV injection of DiD-Lipidots™ in *Nude* mice bearing OVCAR (human ovarian adenocarcinoma), Ts/Apc (murine breast cancer) or HEK β3 (human embryonic kidney cells genetically modified to over-express $\alpha_v\beta_3$ integrins) xenografts. The HEK β3 cell line is an interesting model, since 25% of tumor cell lines over-express $\alpha_v\beta_3$ integrins [13]. Significant particle tumor uptake is observed for the OVCAR and Ts/Apc models, for which tumor growth is rapid (≈ 2 weeks) and EPR effect is assumed to be important.

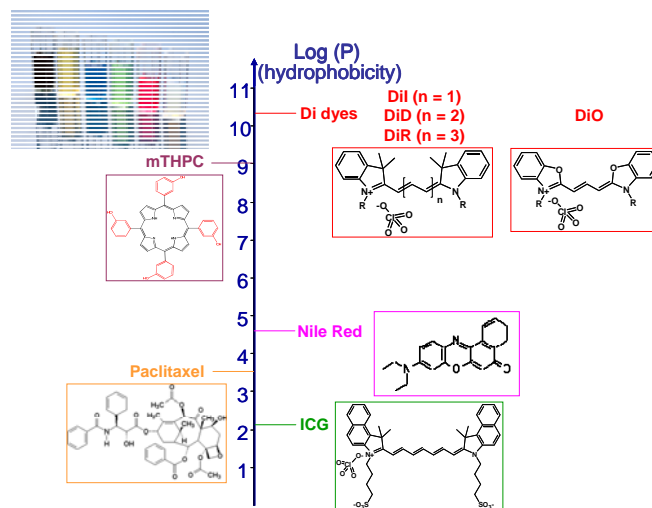


Figure 5: Lipidots™ loading with organic dyes and active pharmaceutical ingredients. On photograph, from left to right: Lipidots™ loaded with mTHPC, paclitaxel, DiD, ICG, Nile Red, and unloaded particles.

On the contrary, HEK β3 tumors grow in ≈ 6 weeks, and no significant particle uptake is observed for non functionalized Lipidots™ 24 hours after injection (Figure 6). However, grafting on the nanoparticle surface of the cRGD peptide exhibiting specific adhesion to $\alpha_v\beta_3$ integrins, improves tumor accumulation of the functionalized lipid nanoparticles, compared to the non functionalized ones (Figure 6) [8].

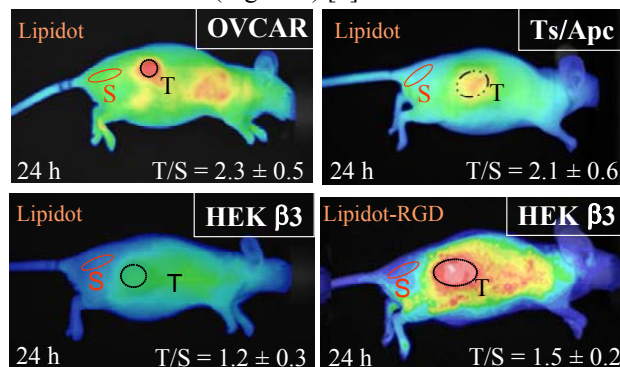


Figure 6: Tumor targeting with Lipidots™. The T/S (tumor over skin fluorescence ratio) values given are mean \pm standard deviation of 3 animals per group.

In vivo specific Lipidots™ tumor targeting and cellular uptake can therefore be achieved. Combined with the ability of the particles to encapsulate a wide range of amphiphilic to lipophilic compounds, such as mTHPC, Paclitaxel and ICG (only near-infrared dye approved for human use until now), different applications can be envisioned in the oncology field, such as diagnostics and imaging, phototherapy and chemotherapy.

3 CONCLUSIONS

Lipidots™, lipid nanoparticles composed of ingredients already approved for human use, are manufactured by ultrasonication, an industry-scaled process. Their long-term stability in storage conditions, their low cytotoxicity and *in vivo* targeting abilities, make them nanocarriers of choice to explore a wide range of imaging and drug delivery applications in oncology.

4 EXPERIMENTAL SECTION

4.1 Lipidots™ Processing

The nanoemulsion processing has already been detailed elsewhere [7-9]. Briefly, lipid phase is prepared by mixing solid (Suppocire NC, Gattefossé) and/or liquid (Super-refined Soybean oil, Croda) glycerides, Lipoid s75 (Lipoid GmbH), and eventually the compound to be loaded in the Lipidots™. The aqueous phase is composed of Myrj s40 (Croda) and aqueous buffer (usually 1X PBS). After homogenization at 45°C, both phases are crudely mixed and sonication cycles are performed for 5 minutes. Non encapsulated components are separated by overnight dialysis (MWCO: 12 kDa). Lipidots™ dispersions are filtered through a 0.22 µm cellulose Millipore membrane before use. Batches of particles with specified diameter can be obtained depending on the lipid and surfactants ratios, as previously described [6, 7, 9].

4.2 Lipidots™ Characterization

The hydrodynamic diameter are measured with a Malvern Zeta Sizer Nano instrument (NanoZS, Malvern, UK) in 0.1 X PBS buffer. DSC thermograms and ¹H NMR spectra have respectively been recorded on a TA Q200 system (TA instrument, France) and a Bruker Avance DPX 500 spectrometer (Bruker, Germany) [6].

4.3 Cytotoxicity Assay

NIH-3T3 murine fibroblast cells (ATCC) are cultured under a humidified (90%) atmosphere of 95% air/ 5 % CO₂ at 37 °C, in Dulbecco's modified Eagle's medium high glucose supplemented with 10% newborn calf serum and 1% penicillin and streptomycin. 5.10⁴ cells/ well are incubated for 24 hours at 37 °C, previous to addition of different amounts of nanoparticles. Cytotoxicity is assessed

24 hours after the nanoparticle treatment followed by two washes with cell culture medium, using WST-1 assay.

4.4 Biodistribution in Healthy Mice

Female FVB mice (Janvier, 18 animals) are injected with 50 nm-diameter Lipidots™ labelled with 0.15% ¹⁴C-cholesteryl oleate (CO) and 0.45% ³H-cholesteryl-hexadecyl-ether (CHE) (Perkin Elmer). Blood samples (20 µL) are collected at sinus, organs are harvested after animal sacrifice. Radioactivity counting is performed on a 2200CA TriCarb Counter (Packard).

4.5 *In Vivo* Tumor Imaging

In vivo tumor imaging experiments have been described elsewhere [8, 9].

REFERENCES

- [1] Maeda H, Wu J, Sawa T, Matsumura Y, Hori K, J Control Release, 65, 271-284, 2000.
- [2] Couvreur P, Vauthier C, Pharmaceutical Res, 23 1417-1450, 2006.
- [3] Torchilin VP, Adv Drug Deliv Rev, 58, 1532-1555, 2006.
- [4] Anton N, Benoit JP, Saulnier P, J Control Release, 128, 185-194, 2008.
- [5] Mehnert W, Mäder K, Adv Drug Deliv Rev, 47, 165-196, 2001.
- [6] Delmas T, Couffin AC, Bayle PA, Crécy Fd, Neumann E, Vinet F, et al., J Colloid Interf Sci, in reviewing.
- [7] Delmas T, Piraux H, Couffin AC, Texier I, Vinet F, Poulin P, et al., Langmuir, 27, 1683-1692, 2011.
- [8] Goutayer M, Dufort S, Josserand V, Royère A, Heinrich E, Vinet F, et al., Eur J Pharm Biopharm, 75, 137-147, 2010.
- [9] Texier I, Goutayer M, Da Silva A, Guyon L, Djaker N, Josserand V, et al., J Biomed Opt, 14, 054005, 2009.
- [10] Poulin P, Bibette J, Phys Rev Lett, 79, 3290-3292, 1997.
- [11] Weyenberg W, Filev P, Van den Plas D, Vandervoort J, De Smet K, Sollie P, et al., Int J Pharm, 337, 291-298, 2007.
- [12] Moghimi SM, Hunter AC, Murray JC, Pharmacol Rev, 53, 283-318, 2001.
- [13] Schottelius M, Laufer B, Kessler H, Wester H-J, Acc Chem Res, 42, 969-980, 2009.